

A nonlinear model to estimate vibration frequencies in surface mines

Mojtaba Mokhtarian-Asl^{a,*}, Aref Alipour^a

^a Faculty of Mining and Metallurgical Engineering, Urmia University of Technology, Urmia, Iran

Article History:

Received: 20 February 2019,

Revised: 17 September 2019,

Accepted: 20 October 2019.

ABSTRACT

Twenty measured blast data from the Golegozar iron mine (southern Iran) were used to generalize nonlinear models for the estimation of dominant frequencies of blast waves using rock mass, explosive characteristics, and blast design. The imperialist Competitive Algorithm (ICA) was used to determine the nonlinear regression model coefficients. Possessing a good correlation coefficient, the proposed model can be directly used for predicting blast-induced dominant frequencies of waves. The determination coefficient (R^2) found by the ACI-based nonlinear model was 0.98 for frequency, while that of the traditional Multivariate Linear Regression Model (MVLRM) was 0.89. Also, according to the calculation of other well-known statistical errors between the estimated and real measured values of frequency, ICA-based models have higher Variance Account for (VAF) value, as well as lower values of Route Mean Square Error (RMSE), Variance Absolute Relative Error (VARE), Median Absolute Error (MEDAE), and Mean absolute percentage error (MAPE) compared to the linear model. It was found that the proposed nonlinear model is more accurate and capable of estimating the values of the dominant frequency of blast waves.

Keywords : Ground vibration, frequency, nonlinear model, Imperialist Competitive Algorithm

1. Introduction

Ground vibrations attenuate the explosive energy that can be used for rock fracturing. Excessive ground vibrations can cause problems to local residents, and also negatively influence the integrity of the structures in the mine area. In order to lessen the problems caused by vibration, different parameters should be taken into account in the design of a blasting pattern. These parameters include explosives specifications, physico-mechanical properties of the rock mass, and geometrical and timing aspects of the blasting pattern [1-3]. Many parameters determine the dispersion of seismic energy, such as delay time, burden, maximum charge per delay, spacing, charge length, initiation sequence, and decoupling charges. The characteristics of rock differ greatly between different mines, or even at different spots of a single face. Therefore, there is a need to optimize the blast design parameters and explosive characteristics depending on rock mass properties, such as its longitudinal wave velocity, impedance, strength, density, porosity, stress-strain response and presence of structural discontinuities [2]. Up until now, not many investigations have tried to understand the relationship between geo-mechanics and blast parameters of ground vibration. A limited number of these investigations have modeled the effect of rock characteristics, explosive characteristics, and blast design. These limited research studies include the use of artificial intelligence-based methods presented in references [2, 4-6].

The use of black-box models, such as artificial neural networks, in construction projects and mining sites, is not possible and requires clearly formulated models. Also, there is no acceptable model for determining the dominant frequency.

One of the standard methods to measure the blast vibration is Peak particle velocity (PPV). This method, however, cannot explain the effects of vibration on the structures (e.g., surface building). Such effects can appear far away from the point of blasting face and even causes damage at the very low PPV. The low-frequency content of ground

vibration, according to the recorded spectral analysis of vibration, can inflict serious damages to the structures in comparison to the high-frequency one.

Vibration standards recognize that the potential for damage from vibration strongly depends on the frequencies of the vibration. They set different "allowable" vibration intensities for different frequencies of vibration. Therefore, determining the frequencies and intensities that support the overall vibration is imperative for achieving a deeper knowledge of potential damages [7].

The main objectives of the present study are applying the ICA-based nonlinear model to measure the blast vibration main frequencies, as well as comparing the results with those of the MVLRM. The data used in this study belong to the Golegozar iron mine, to which the MVLRM was applied to determine the statistical characteristics. The obtained dominant frequencies of the blast vibration were compared with the results of ICA-based nonlinear models.

2. Blast-induced vibration quantification

By detonating an explosive charge in a blast hole, instant dynamic stresses are generated by the sudden acceleration of the rock mass in borehole walls. When the stress wave travels through the surrounding rocks, a motion wave is generated within the ground. Due to the strain energy impact transmitted by these waves, the rocks break with a variety of breaking mechanisms, including crushing, radial cracking, and reflection breakage in the presence of a free face. The stress wave travels in the form of elastic waves in the medium. As a result, the wave oscillates the particle in the medium in which it travels. Within the elastic zone, these waves are called PPV, which have a close confirmation of the viscoelastic behavior. The wave spreads concentrically from the blast site in all directions and gradually loses its energy by spreading a fixed amount of energy over an area from its origin [6]. All these parameters play a key role in blast design, and changing them may cause notable changes in the amplitude and

* Corresponding author. E-mail address: m.mokhtarian@uut.ac.ir (M. Mokhtarian-Asl).

frequency of the blast vibration. The PPV is a standard way to examine blast vibration damage potential. However, this parameter is not robust enough to describe the effect on structures, such as surface buildings, positioned in far distances from the point of blasting, which can be destroyed even at very low PPVs. According to spectral analysis, low-frequency ground vibrations cause more intense damages than high frequencies [8, 9]. In the case of blasts in mines, the frequency is usually below 100 Hz for mining blasts, and it does not exceed 250 Hz even in the case of construction blasts. When an initial disturbance inflicts, it vibrates at one or more of its natural frequencies, on which the mass and stiffness distribution have the main effect. Therefore, it is notable that the degree of structural damage is a function of the closeness of the natural frequency between the structure and earthquake exciting forces and the duration of earthquake ground acceleration [10, 11].

Different ground vibration standards can study different vibration environments and building types. The majority of such standards rely on the frequency dependence of the vibration damage potential. Also, more rigorous standards are set for lower frequency vibrations close to the structure resonance frequencies than at higher ones [12].

2.1. Case study

The Golegohar Iron Mine is located in the Kerman province, Southern Iran. The mine is formed within the Kheir-Abad anticline, which is part of the Sanandaj-Sirjan zone. The lithological units in the mine area include Paleozoic metamorphic rocks in the south and Mesozoic and Cenozoic sedimentary rocks in the east. The Paleozoic metamorphic rocks comprise the Golegohar complex, which is the oldest metamorphic setting that supplies iron ore. The lower division of the complex is a sequence of gneiss, mica schist, amphibolite, and quartz-schist [13,14]. The deposit has six giant anomalies, in the first of which the extraction operation is open-pit mining. This anomaly, which is called Mine I, is excavated through the drill and blast method. Fig. 1 illustrates the operating pit and its location on the geographical map of Iran. Because of the complex discontinuity, diversity of lithological units, and aquifers, it is important to evaluate the blast-induced ground vibration in Golegohar.

Several factors determine the nature and intensity of blast-induced ground vibrations. The peripheral rock types are moderate factors in ground vibration behavior. Geological discontinuity, on the other hand, has a critical role in the transmission of ground vibration [2, 15].

Another effective parameter is the distance between the blast face and vibration monitoring point. Blast geometry, as well, has a critical effect on ground vibration. Other key parameters that can minimize ground vibration under the control level include charge per delay, burden, spacing, charge length, hole diameter, length of the hole, and the like [1].

The main explosive used in the mine is ammonium nitrate and fuel oil (ANFO); however, drilling cuttings are used for the stemming object in Golegohar mine. The first and second rows of blasting are initiated with a delay of 80 ms, and the delay time between other rows was 50 ms. The diameter of blast holes is 251 mm, and every blast hole is drilled using perpendicularly drilled rotary machines. Database properties used in this study and the range of the variables are listed in Table 1.



Fig. 1. Location of the Golegohar iron mine on the geographical map of Iran, and a view of the open-pit mine.

3. Estimation of ground vibration frequency by a multivariate nonlinear model

This section investigates the correlations between blasting properties (B, S, CHL, EPD, D, BI & P) and actual measured frequency by using an ICA-based multivariate nonlinear regression model.

Table 1. The range of blasting parameters in this study.

| Parameter | Index | Range |
|---|-------|--------------|
| Burden (m) | B | 3 – 10.5 |
| Spacing (m) | S | 3.8 – 10.5 |
| Charge length (m) | CHL | 4 – 17.5 |
| Explosive per delay equivalent to ANFO (kg) | EPD | 1600 – 25000 |
| Distance of monitoring point from blasting face (m) | D | 200 – 2800 |
| Blastability Index | BI | 6.2 – 12.9 |
| P-wave velocity (km/s) | P | 1.85 – 3.9 |
| Frequency (Hz) | Fr | 6.2 – 22.7 |

3.1. Imperialist competitive algorithm

The novel imperialist competitive algorithm, which is a population-based meta-heuristic method, was introduced by Atashpaz-Gargari and Lucas (2007). The algorithm copies the socio-political process of imperialism and imperialistic competition [16]. The algorithm's capability to deal with diverse optimization problems has been supported by many studies [17]. Like other evolutionary algorithms, ICA begins with an initial number of solutions that are called countries. Each solution represents the concept of a nation and reflects the quality of the objective function in each solution. The best solutions or countries are elected as *imperialists*, and the remaining solutions are categorized as the 'colonies' of those imperialists. An imperialist and the colonies form an 'empire' [18]. Gradually, imperialists seek to extend their characteristics to the colonies under their control. Still, the procedure is not fully controlled, and revolutions are expected. Countries may also leave one empire in order to join another provided that the new one gives them more chance of promotion. ICA is widely utilized to form different types of optimization problems. For instance, this method is widely employed in stock market forecasting [19], multi-objective optimization [22], designing digital filters [20], traveling salesman problems [21], integrated product mix-outsourcing problems [23], production planning of open-pit mines [24], and scheduling problems [25, 26].

Fig. 2 illustrates a flowchart of the imperialist competitive algorithm. The methodology and implementation of ICA are presented step by step as follows:

Step 1- Generating the initial empires: an optimization algorithm starts with an initial population consisting of N_{pop} solutions including N_{imp} of the strongest ones that represent the imperialists. The remaining member of the population ($N_{col} = N_{pop} - N_{imp}$) represent the colonies of the empires. The primary empires and colonies are divided among the imperialists, given their power as the higher the power of an empire, the more the colonies covered by it. Equation 1 tries to distribute the colonies among imperialists based on their power and to obtain the normalized cost of the n^{th} imperialist, as follows [23]:

$$C_n = \max \{c_i\} - c_n, \quad i = 1, 2, \dots, N_{imp} \quad (1)$$

Where c_n and C_n represent the cost and the normalized cost of n^{th} imperialist, respectively. Therefore, each imperialist's normalized power is determined as follows [23]:

$$pow_n = \left| C_n / \sum_{i=1}^{N_{imp}} C_i \right| \quad (2)$$

The number of colonies controlled by an imperialist is determined by its normalized power. Therefore, the count of colonies of an empire at the beginning is given as [23]:

$$ColEmp_n = \text{round}(pow_n \times N_{col}) \quad (3)$$

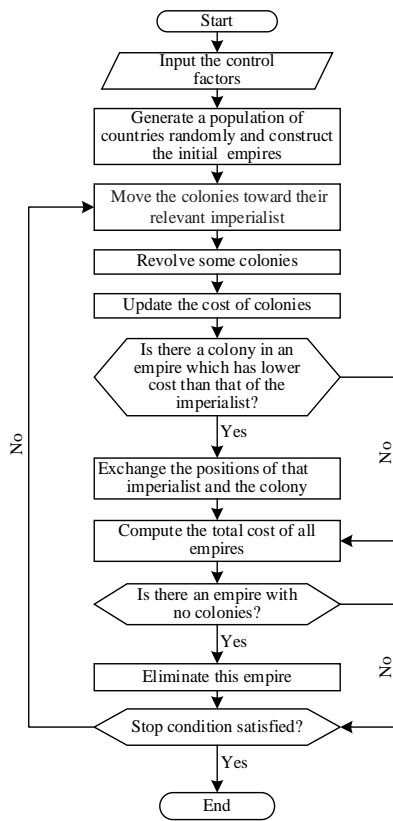


Fig. 2. Flowchart of the imperialist competitive algorithm.

Where, $ColEmp_n$ is the starting number of colonies of the n^{th} empire determined in the whole colony population randomly.

Step 2- Assimilation process: The colony can move toward the imperialist on a different socio-political axis like culture and language. The colony can approach the imperialist by x units while x stands for a random number with a uniform distribution

Step 3- Revolution: The operator diversifies ICA to examine new regions. The mechanism protects the algorithm from being trapped in local optima [27]. Therefore, each iteration selects the weakest colony and randomly replaces it with a new one.

Step 4- Imperialist and a colony substitution: A colony can reach the position where the cost function is less than that of its imperialist. When this happens, the colony and imperialist replace their position.

Step 5- Calculating the total power of an empire: It is obtained based on the power of its imperialist country; while, the powers of its individual colonies also have an important influence, which is relatively insignificant. Therefore, the total cost of an empire is as [17]:

$$TC_n = \text{cost}(\text{imperialist}_n) + \xi \text{mean}(\text{cost}(\text{colonies of empire}_n)) \quad (4)$$

Where TC represents the total cost of the n^{th} empire and ξ stands for the positive number that is considered less than 1.

Step 6- Imperialistic competition: In order to model the competition, one of the weakest colonies of the weakest empires is selected, and competition is triggered among all empires to control this colony. This chance of each colony to possess each empire is relative to the total power. The normalized total cost of each empire is determined as [17]:

$$NTC_n = \max\{TC_i\} - TC_n \quad i = 1, 2, \dots, N_{imp} \quad (5)$$

Where TC_n and NTC_n represent the total cost and the normalized total cost of the n^{th} empire, respectively. Now, the chance of possession for each empire is given by [17]:

$$p_n = \left| \frac{NTC_n}{\sum_{i=1}^{N_{imp}} NTC_i} \right| \quad (6)$$

Vector P is formed to determine the share of each empire of the noted colonies, as follows [17]:

$$P = [p_1, p_2, p_3, \dots, p_{N_{imp}}] \quad (7)$$

Afterward, vector R equal to P in size is created, of which the elements are some uniformly distributed random numbers between 0 and 1.

$$R = [r_1, r_2, r_3, \dots, r_{imp}], \quad r_1, r_2, r_3, \dots, r_{imp} \sim U(0, 1) \quad (8)$$

Then, vector D is formed by subtracting R from P .

$$D = P - R = [d_1, d_2, d_3, \dots, d_{N_{imp}}] = [p_1 - r_1, p_2 - r_2, p_3 - r_3, \dots, p_{N_{imp}} - r_{N_{imp}}] \quad (9)$$

Based on vector D , the colonies subject to an empire of which the corresponding index in D is highest will win the possession competition [17].

Step 7- Removing the empires without power: Empires without power will not survive in the imperialistic competition, and their colonies are taken by other empires. Here, an empire falls when all its colonies are lost [17].

Step 8- Stopping criteria: When no iteration remains, or only one empire controls the whole world, the algorithm stops.

3.2. Estimating frequency using ICA

The Fr prediction models were developed using the ICA optimization technique. The new nonlinear estimation model was proposed. ICA has used to determine the nonlinear model coefficients. A method that is appropriate for this procedure is called the nonlinear least-squares fitting. This process minimizes the value of the Mean Squared Error (MSE) of the difference between estimated and measured values. The MSE was selected as the objective function to be decreased to its minimum value. The objective function (MSE) is as follows:

$$\text{Minimize} \quad \frac{1}{n} \sum_{i=1}^n (Fr_{Est} - Fr_{Meas})^2 \quad (10)$$

Fr_{Meas} is the observed and measured Fr , Fr_{Est} is the estimated Fr using the model, and n is the number of observations. In fact, in the ICA model, the fitness function is the total error given by equation (10), which should be minimized, and so it can be written in an extended form with following notations as:

$$\text{Minimize} \quad \sum_{i=1}^n \left(\left| k_0 + k_1 \times B_i^{k_2} \times S_i^{k_3} \times CHL_i^{k_4} \times EPD_i^{k_5} \times D_i^{k_6} \times BI_i^{k_7} \times P_i^{k_8} \right| - Fr_{Meas} \right)^2 \quad (11)$$

Different variables related to the equation (11) were introduced in previous sections. The estimated Fr , Fr_{Est} values are as follows:

$$Fr_{Est} = \left| k_0 + k_1 \times B_i^{k_2} \times S_i^{k_3} \times CHL_i^{k_4} \times EPD_i^{k_5} \times D_i^{k_6} \times BI_i^{k_7} \times P_i^{k_8} \right| \quad (12)$$

In order to use the ACI optimization method, in this work, the C++ program was used to model and estimate Fr . Afterward, the optimized values were achieved for the constants of nonlinear regression. Based on the analysis, the optimum equation obtained from ACI-based is formulated in equation 13.

$$Fr_{Est_{ICA}} = \left| 7.438 + 309.893 \times B_i^{3.711} \times S_i^{1.491} \times CHL_i^{19.951} \times EPD_i^{-11.282} \times D_i^{0.649} \times BI_i^{-0.068} \times P_i^{2.547} \right| \quad (13)$$

The same data were used to estimate Fr by using the multivariate linear regression model, which is commonly used for such problems. To obtain the constants coefficients, all 20 sets of data were transferred in the Microsoft Excel program, and their relationship was found to be as:

$$Fr_{Est_{MVLRLM}} = -3.198 - 0.005B - 1.495S + 0.872CHL - 0.011EPD + 1.196D - 0.759BI + 2.944P \quad (14)$$

A comparison of the measured and estimated outputs from the ICA-based model and the MVLRLM are presented in Fig. 3. The diagonal index line indicates the perfect goodness of fit. As shown by the result, the estimated inflections are coincident to the measured ones. The coefficient of correlation was high for the proposed ACI-based estimator in comparison to the MVLRLM and provided a better prediction of Fr for

the case study. The distribution of event points around the regression diagonal index line is more scattered for the MVLRM.

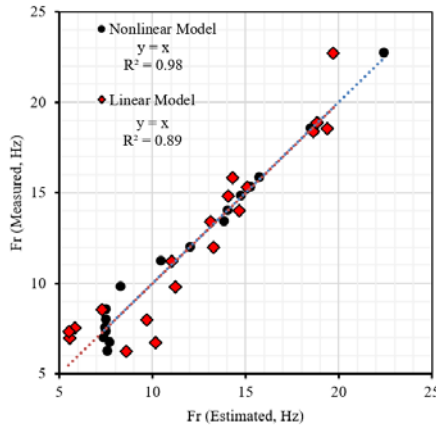


Fig. 3. Correlation between the measured and estimated frequency values for the ACI and MVLRM models.

3.3. Results and discussion

The performance of different predictor models can be controlled by the Route Mean Square Error (RMSE), Variance Absolute Relative Error (VARE), Median Absolute Error (MEDAE), Mean Absolute Percentage Error (MAPE), and Variance Account for (VAF). The formulation of these indices can be found in Table 2.

The ACI-based model with a higher determination coefficient and VAF value as well as lower RMSE, VARE, MEDAE, and MAPE values show a better performance. The results of the assessment, according to the statistical goodness criteria for the mentioned regressions, are presented in Table 3.

Table 2. Statistical criteria controlling the performance of estimator models.

| Statistical criteria | Formulation |
|--|--|
| Route Mean Square Error, (RMSE) | $RMSE = \sqrt{\frac{1}{n} \times \sum_{i=1}^{i=n} (Fr_{Meas} - Fr_{Est})^2}$ |
| Variance Absolute Relative Error, (VARE) | $VARE = \text{var} \left(\frac{Fr_{Meas} - Fr_{Est}}{Fr_{Meas}} \right) \times 100$ |
| Median Absolute Error, (MEDAE) | $MEDAE = \text{median} \left(\frac{Fr_{Meas} - Fr_{Est}}{Fr_{Meas}} \right)$ |
| Mean absolute percentage error, (MAPE) | $MAPE = \frac{1}{n} \times \sum_{i=1}^{i=n} \left \frac{Fr_{Meas}^i - Fr_{Est}^i}{Fr_{Meas}^i} \right $ |
| Variance Account for, (VAF) | $VAF = \left[1 - \frac{\text{var}(Fr_{Meas} - Fr_{Est})}{\text{var}(Fr_{Meas})} \right] \times 100$ |

Table 3. Results of regression goodness according to the statistical criteria.

| Model | RMSE | VARE | MEDAE | VAF | MAPE |
|---|-------|-------|-------|--------|--------|
| Multivariate linear model | 1.574 | 1.800 | 0.105 | 89.400 | 13.818 |
| ICA-based multivariate non-linear model | 0.624 | 0.406 | 0.018 | 98.336 | 4.948 |

4. Conclusion

Blast vibration standards indicated that the capacity for damage highly depends on the frequencies of blast waves. Different "allowable" vibration intensities are set for different vibration frequencies. The feasible levels are represented based on the peak particle velocity and the dominant frequencies. Explosion engineers should control ground vibrations to make sure that the vibrations remain at permissible levels. This research offered a nonlinear model for dominant wave frequencies by considering rock mass parameters, explosive characteristics, and the

blast design. The imperialist competitive algorithm was used to find the coefficients of the frequency estimator model. Based on the prediction results, the squared correlation coefficient (R²) between the observed and predicted values of the proposed model was obtained 0.98, indicating strong conformity between the predicted and actual penetration rates. The ACI-based model with higher VAF as well as lower MAPE, RMSE, VARE values showed a better performance. The output of the proposed model covered the effects of ground vibration frequencies and indicated the permissible peak particle velocity to control the blast. Therefore, the suggested method is capable of being applied in similar cases.

REFERENCES

- [1] Hossaini, S. and Sen G. (2004). Effect of explosive type on particle velocity criteria in ground vibration. Journal of Explosives Engineering, 21(4), 34-36.
- [2] Khandelwal, M. and Singh T.N. (2006). Prediction of blast induced ground vibrations and frequency in opencast mine: A neural network approach. Journal of Sound and Vibration, 289(4), 711-725.
- [3] Bakhshandeh Amnieh, H., Siamaki A., and Soltani S. (2012). Design of blasting pattern in proportion to the peak particle velocity (PPV): Artificial neural networks approach. Safety Science, 50(9), 1913-1916.
- [4] Khandelwal, M. and Singh T.N. (2009). Prediction of blast-induced ground vibration using artificial neural network. International Journal of Rock Mechanics and Mining Sciences, 46(7), 1214-1222.
- [5] Q. Yuan, L. Wu, Qingjun Zuo, and Li B. (2014). Peak particle velocity and principal frequency prediction based on RS-FNN comprehension method for blasting vibration. Electronic Journal of Geotechnical Engineering, 19, 10043-10056.
- [6] Singh, T. and Singh V. (2005). An intelligent approach to prediction and control ground vibration in mines. Geotechnical & Geological Engineering, 23(3), 249-262.
- [7] Mines, U.S.B.o. and Siskind D. (1980). Structure response and damage produced by ground vibration from surface mine blasting. US Department of the Interior, Bureau of Mines New York.
- [8] Singh, T., Singh A., and Singh C. (1994). Prediction of ground vibration induced by blasting. Indian Min Eng J, 31-34(33), 16.
- [9] Singh, T. (2004). Artificial neural network approach for prediction and control of ground vibrations in mines. Mining Technology, 113(4), 251-256.
- [10] Berta, G. (1994). Blasting-induced vibration in tunnelling. Tunnelling and Underground Space Technology, 9(2), 175-187.
- [11] Adhikari, G. and Singh R. (1989). Structural response to ground vibration from blasting in opencast coal mines. Journal of Mines, Metals & Fuels, 37(4), 135-138.
- [12] Singh, T.N. and Verma A.K. (2010). Sensitivity of total charge and maximum charge per delay on ground vibration. Geomatics, Natural Hazards and Risk, 1(3), 259-272.
- [13] Saeidi, O., Torabi S.R., Ataei M., and Rostami J. (2014). A stochastic penetration rate model for rotary drilling in surface mines. International Journal of Rock Mechanics and Mining Sciences, 68, 55-65.
- [14] Kamkar-Rouhani, A. and Hojat A.). Determination of groundwater and geological factors using geoelectrical methods to design a suitable drainage system in Gol-e-Gohar iron ore

mine, Iran.

- [15] Singh, D. and Sastry V. (1986). Rock fragmentation by blasting influence of joint filling material. *Journal of Explosive Engineering*, 18-27.
- [16] Khabbazi, A., Atashpaz-Gargari E., and Lucas C. (2009). Imperialist competitive algorithm for minimum bit error rate beamforming. *International Journal of Bio-Inspired Computation*, 1(1-2), 125-133.
- [17] Atashpaz-Gargari, E. and Lucas C. (2007). Imperialist competitive algorithm: an algorithm for optimization inspired by imperialistic competition. in *Evolutionary computation, 2007. CEC 2007. IEEE Congress on. IEEE*, 4661-4667.
- [18] Shokrollahpour, E., Zandieh M., and Dorri B. (2011). A novel imperialist competitive algorithm for bi-criteria scheduling of the assembly flowshop problem. *International Journal of Production Research*, 49(11), 3087-3103.
- [19] Sadaei, H.J., Enayatifar R., Lee M.H., and Mahmud M. (2016). A hybrid model based on differential fuzzy logic relationships and imperialist competitive algorithm for stock market forecasting. *Applied Soft Computing*, 40, 132-149.
- [20] Sharifi, M.A. and Mojallali H. (2015). A modified imperialist competitive algorithm for digital IIR filter design. *Optik - International Journal for Light and Electron Optics*, 126(21), 2979-2984.
- [21] Ardalan, Z., Karimi S., Poursabzi O., and Naderi B. (2015). A novel imperialist competitive algorithm for generalized traveling salesman problems. *Applied Soft Computing*, 26, 546-555.
- [22] Maroufmashtat, A., Sayedin F., and Khavas S.S. (2014). An imperialist competitive algorithm approach for multi-objective optimization of direct coupling photovoltaic-electrolyzer systems. *International Journal of Hydrogen Energy*, 39(33), 18743-18757.
- [23] Nazari-Shirkouhi, S., Eivazy H., Ghodsi R., Rezaie K., and Atashpaz-Gargari E. (2010). Solving the integrated product mix-outsourcing problem using the Imperialist Competitive Algorithm. *Expert Systems with Applications*, 37(12), 7615-7626.
- [24] Mokhtarian Asl, M. and Sattarvand J. (2016). An imperialist competitive algorithm for solving the production scheduling problem in open pit mine. *Int. Journal of Mining & Geo-Engineering*, 50(1), 131-143.
- [25] Behnamian, J. and Zandieh M. (2011). A discrete colonial competitive algorithm for hybrid flowshop scheduling to minimize earliness and quadratic tardiness penalties. *Expert Systems with Applications*, 38(12), 14490-14498.
- [26] Lian, K., Zhang C., Gao L., and Shao X. (2012). A modified colonial competitive algorithm for the mixed-model U-line balancing and sequencing problem. *International Journal of Production Research*, 50(18), 5117-5131.
- [27] Mortazavi, A., Khamseh A.A., and Naderi B. (2015). A novel chaotic imperialist competitive algorithm for production and air transportation scheduling problems. *Neural Computing and Applications*, 26(7), 1709-1723.